

Parametric Studies of Adaptive Optics by Self-Interference Incoherent Digital Holography

Jisoo Hong and Myung K. Kim

Department of Physics, University of South Florida, Tampa, FL, US 33620

ABSTRACT

Adaptive optics (AO) in astronomical imaging is a technique to improve the quality of image by compensating aberrations induced by atmospheric turbulence. Digital holographic AO (DHAO) is one attractive option to implement AO scheme because it is capable of directly measuring the phase profile of aberration without complicated calculation or loss of resolution of CCD. Hence, if applicable, DHAO is expected to have advantages over traditional AO systems. Recent development of self-interference incoherent digital holography (SIDH) makes it possible to apply the concept of DHAO for an astronomical application where the illumination is incoherent and cannot be controlled. We have investigated the image characteristics according to various parameters of SIDH AO to derive optimum condition or design of the system. We observe not only well-known super-resolution property of SIDH but also interesting and significant improvement of noise behavior by aberration compensation. Because of many beneficial features, we expect that SIDH AO will be a useful tool for astronomical imaging.

Keywords: incoherent digital holography, adaptive optics, astronomical imaging, aberration compensation

1. INTRODUCTION

Adaptive optics (AO) technique was first developed for astronomical imaging to compensate atmospheric turbulence to acquire clearer images. The aberration induced by turbulence is measured by Shack-Hartmann or pyramid wavefront sensor from guide-star [1]. Based on the measured information, the aberration is compensated using dynamic devices such as deformable mirror or spatial light modulator in real time. AO is also useful for ophthalmic application [2] because the aberration of cornea can degrade the image quality when the structure inside human eye is investigated. Especially, when very small structures such as retinal cells are to be investigated, the effect of aberration is more significant and AO is indispensable. Hence, many ophthalmic applications such as scanning laser ophthalmoscopy [3] and optical coherence tomography [4] are adopting AO technique.

Adoption of digital holography (DH) can make the implementation of AO easier because DH is capable of measuring a phase profile directly [5]. Creating an artificial guide-star, the phase-profile of aberration can be estimated from the recorded guide-star hologram without a feedback loop. Hence, it is possible to compensate the aberration of recorded full-field hologram by post-processing. Moreover, the recorded guide-star hologram uses full resolution of the camera unlike other common wavefront sensors, which will be helpful for better performance of AO. However, DH technique requires use of coherent illumination source and it limits the application of DHAO because: 1) speckle noise induced by laser degrades the image quality; 2) illumination to the entire FOV should be controllable. Especially, the second problem makes it impossible to apply DHAO for astronomical imaging.

Recently, with the development of electronic devices and computer science, various schemes are developed to record holographic information under the incoherent illumination [6-9]. Self-interference incoherent digital holography (SIDH) is one of those techniques which can successfully record holographic information from incoherently illuminated object [8, 9]. Because SIDH does not require any limitation to the illumination, holographic information can be recorded even under the sunlight. Our group has reported the implementation of full-color holographic camera which can record the natural outdoor scene recently [8]. And the holographic information also can be recorded from self-luminous objects. Rosen *et al.* reported about development of holographic microscope applicable for fluorescence object [9]. Hence, by applying SIDH for AO, recording guide-star hologram and compensation of aberration from full-field hologram can be done for the applications where the conventional coherent holographic imaging could not be used.

In this paper, we discuss about the application of SIDH AO for the astronomical imaging. The optical configuration of SIDH AO is described and the optimal conditions to design system parameters will be discussed. The performance of

aberration compensation can be varied according to various parameters. SNR and resolution are investigated and compared to understand the effectiveness of SIDH AO for astronomical imaging.

2. CONFIGURATION OF SELF-INTERFERENCE INCOHERENT DIGITAL HOLOGRAPHY FOR ADAPTIVE OPTICS

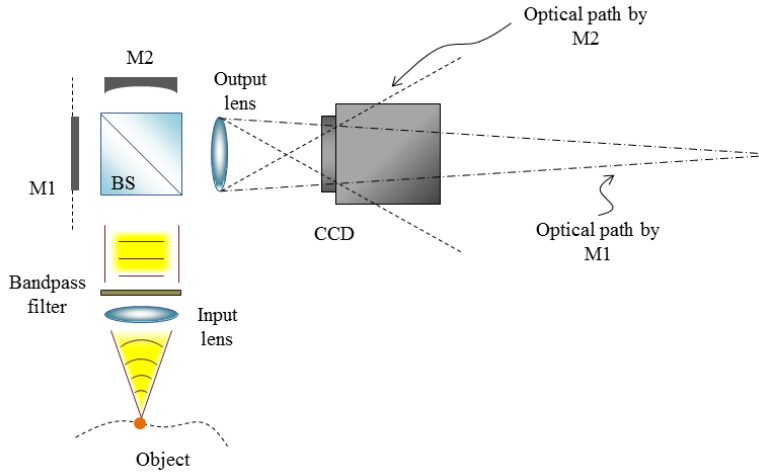


Figure 1. Brief optical configuration of SIDH. M1: plane mirror; M2: curved mirror; BS: beam splitter

Figure 1 shows one of common optical configurations to implement SIDH scheme. Light emanated from each point on the object plane is first imaged by an input lens of the system. Usually the distance between object plane and input lens is set to be close to a focal length of input lens to make it functioning as an infinity corrected objective. Then the light is separated by a beam splitter to two copies of beams and reflected by two different mirrors. Those two mirrors impose different curvatures to wavefront of each beam. Then those two beams interfere with each other to create interferogram on the CCD plane. Use of an output lens gives flexibility in determining the location of CCD. Considering the contribution from all the points on the object plane, the entire interferogram is obtained by adding up all the interferograms of point sources. To remove the DC term of recorded interferogram and retrieve the complex hologram, three or four steps of phase-shift is usually adopted. By moving one of mirrors using a piezo-actuator, a phase-shifting interferometry can be easily implemented. After conversion to the complex hologram, the contribution from each point source becomes a quadratic phase function. Hence, a simple Fresnel propagation of achieved complex hologram can reconstruct object image computationally.

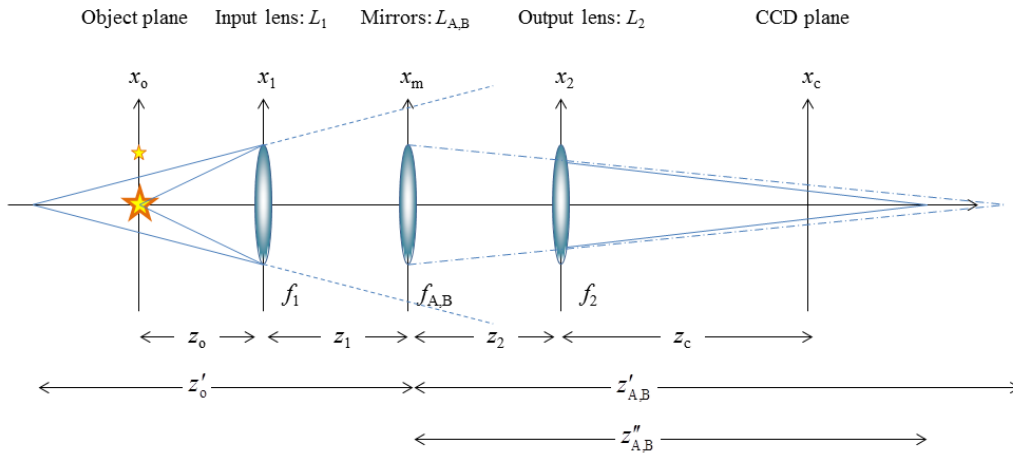


Figure 2. Geometry to analyze the optical configuration presented in Fig. 1.

SIDH configuration shown in Fig. 1 can be interpreted as conceptual diagram shown in Fig. 2 (without any loss of generality, only x -axis in lateral direction will be considered for further discussion). For easier understanding, each mirror has been alternated to lens with same focal length (on plane x_m in Fig. 2). Hence, two different optical paths, which were 90° folded in the original configuration because of reflection, could be straightened and overlapped on the same axis. Instead of letting one of mirrors to be a plane mirror, both of mirrors were considered to have certain curvatures in this analysis. On the plane x_m , f_A and f_B represent focal lengths of two different mirrors respectively. The input lens images the object plane to the virtual plane located at z'_o far from the input lens where

$$z'_o = z_1 - \frac{z_o f_1}{z_o - f_1}. \quad (1)$$

If we first consider the optical path by reflection of mirror with focal length f_A , it will be imaged at the plane located z'_A far from the mirror where

$$z'_A = \frac{z'_o f_A}{z'_o - f_A}. \quad (2)$$

Finally, it will be imaged by the output lens at the plane located z''_A far from the output lens where

$$z''_A = \frac{(z'_A - z_2) f_2}{(z'_A - z_2) + f_2}. \quad (3)$$

For the other optical path (optical path by reflection of mirror with focal length f_B), every parameters can be calculated in the same way by simply changing f_A to f_B . To obtain nice and clean interference pattern on the CCD plane, optical powers separated by mirrors (i.e. L_A and L_B in Fig. 2) should be equally spread on CCD pixel. In other words, images of aperture of L_A (or L_B) should occupy same size on CCD plane. Neglecting the effect of aperture of the output lens, the magnification of aperture image on CCD plane will be:

$$\frac{(z'_A - z_2)(z_c - z''_A)}{z'_A z''_A} \quad (4)$$

for the first optical path, and

$$\frac{(z'_B - z_2)(z_c - z''_B)}{z'_B z''_B} \quad (5)$$

for the second optical path. Hence, the CCD position should be decided in a way satisfying the condition:

$$\frac{(z'_A - z_2)(z_c - z''_A)}{z'_A z''_A} = \frac{(z'_B - z_2)(z_c - z''_B)}{z'_B z''_B} \quad (6)$$

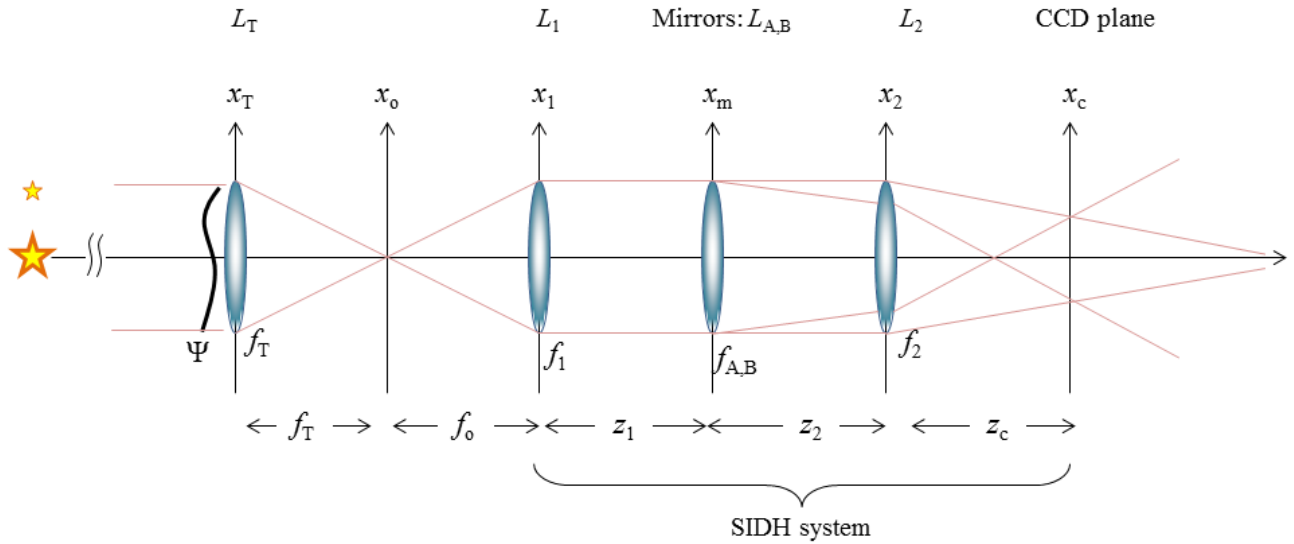


Figure 3. Optical configuration to apply SIDH AO for astronomical imaging.

Figure 3 shows the optical configuration to apply SIDH AO for the astronomical application. In front of SIDH setup discussed in Fig. 2, the additional lens is located to collect the light coming from stars and make an image of them. The image plane will be created at the focal length of the additional lens, f_T . SIDH system is located f_1 far from this image plane to make every calculation simpler. Assuming that the aberration is contributed on the surface of the additional lens L_T , this aberration should be imaged on the surface of mirrors to use the schemes discussed in [10] directly. The condition for this is:

$$z_1 = \frac{(f_T + f_1) f_1}{f_T}. \quad (7)$$

Hence, the system parameters should be designed to satisfy both Eq.(6) and Eq.(7).

3. EFFECTS OF ABERRATION COMPENSATION

Using the optical configuration shown in Fig. 3 and following the design principle introduced throughout Sec. 2, we have simulated the entire process of SIDH AO to study the parameters related to image quality. We have compared the final images obtained by SIDH AO, SIDH without AO, and direct imaging by blocking mirror L_B for various cases (those final images are indicated as \hat{I}_h , I_h , and I_2 respectively). For factors degrading the image quality, we have considered an aberration (characterized by a_ψ , the strength of aberration) and a camera noise (η). Figure 4 shows some examples of phase profile of aberration according to different a_ψ values.

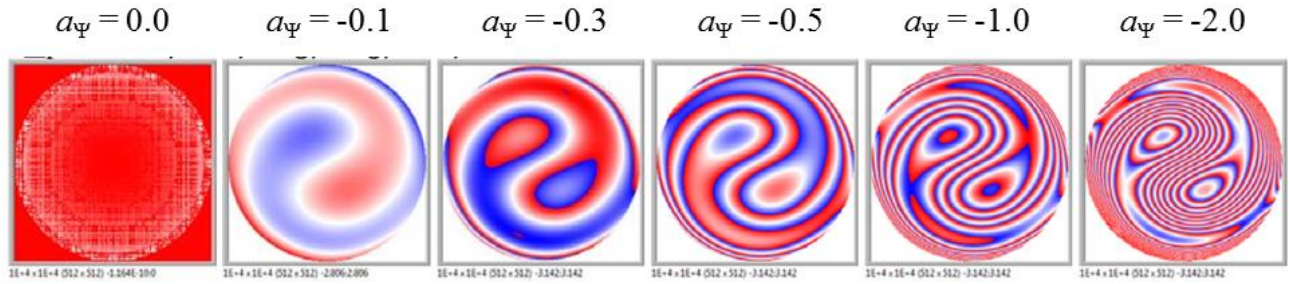


Figure 4. Phase profile of aberration according to various a_ψ values.

Figure 5 shows the effect of noise and aberration to the interferogram recorded by proposed SIDH AO system. As shown in Fig. 5(a), the interferogram without aberration is supposed to show clear Fresnel ring patterns. However, the aberration deteriorates the shape of each Fresnel ring pattern, which will eventually degrade the quality of final image. Figure 5(b) shows the degradation of interferogram according to the noise level.

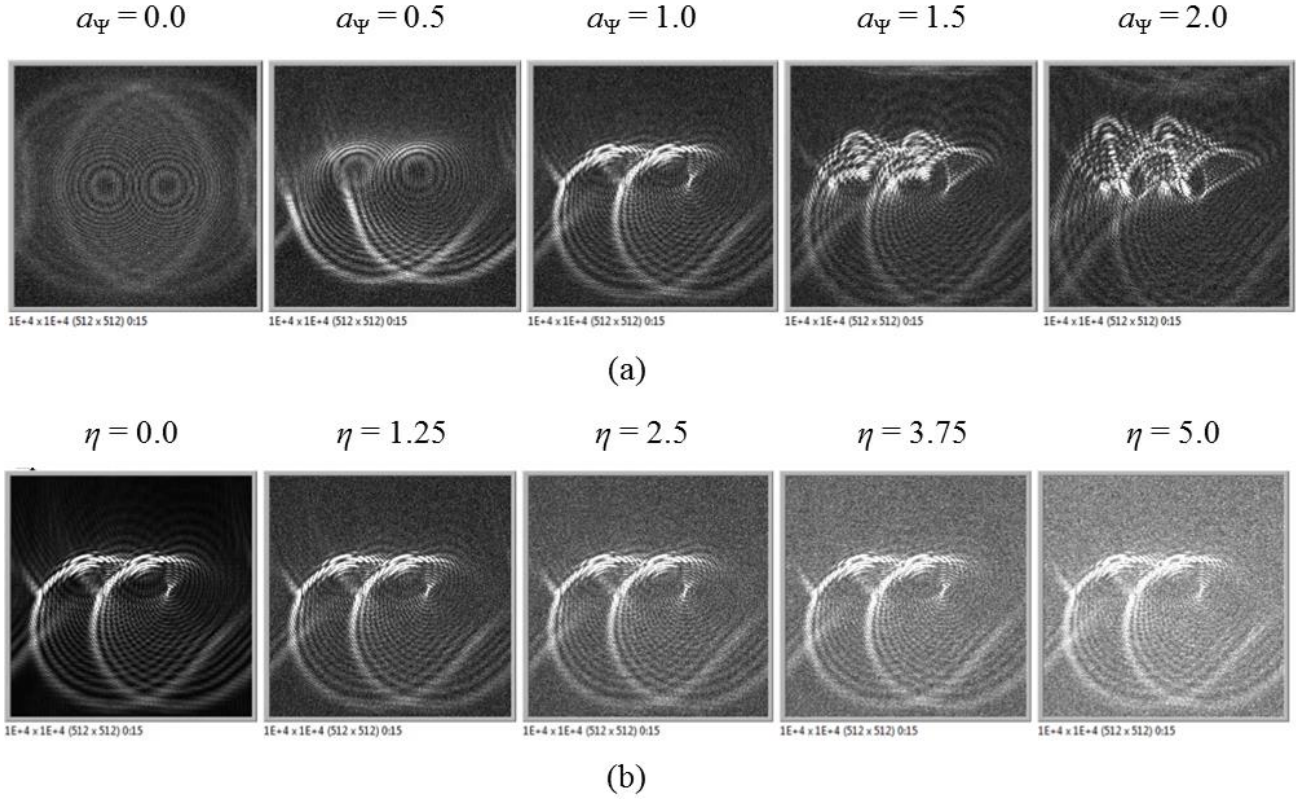
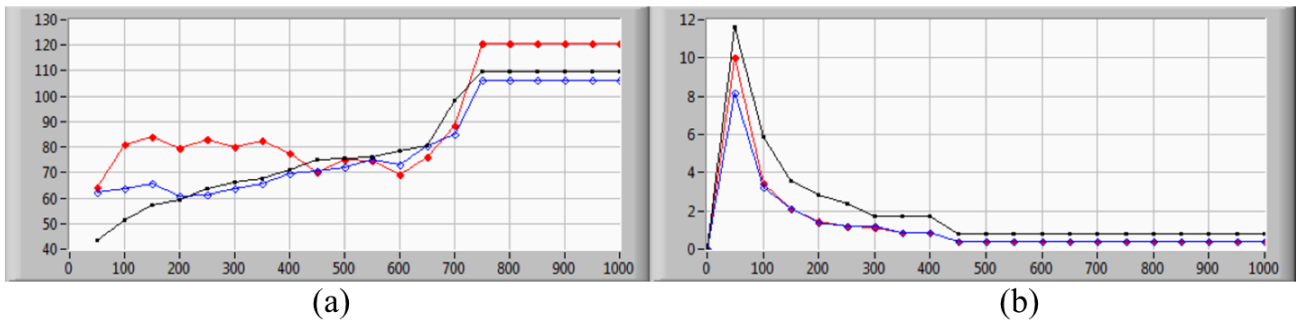


Figure 5. Effect of (a) aberration and (b) noise to the interferogram recorded by CCD.

We compared and investigated SNR and FWHM of I_2 , I_h and \hat{I}_h under various conditions as shown in Fig. 6. Left column of Fig. 6 is SNR variation according to various parameters while right column is variation of FWHM of point spread function. In the first row of Fig. 6, SNR and FWHM of point spread function have been investigated by changing the aperture size of the input lens, under the condition without aberration. The resolution of SIDH is always twice higher than direct imaging of the object which corresponds to the super-resolution property of SIDH itself [11]. The opening of input aperture also affects to the resolution of the reconstruction. The size of aperture of L_T improves SNR (see Fig. 6(a)) and FWHM (Fig. 6(b)) in inverse proportions as easily expected. The saturations of Fig. 6(a) and (b) indicate that it has reached to pixel resolution of CCD. From the second to fifth rows of Fig. 6, the effect of varying aberration strength had been investigated for different noise levels (second and fourth rows: $\eta = 2.5$; third and fifth rows: $\eta = 5.0$) and guide-star intensities (second and third rows: $I_g = 1.0$; fourth and fifth rows: $I_g = 10.0$). Presence of noise and aberration significantly degrades SNR and FWHM. And it is easy to expect that stronger aberration will lower SNR more. The second and third rows of Fig. 6 The interesting investigation is that SNR of \hat{I}_h is not significantly degraded compared to I_2 and I_h . For some cases, SNR is even improved (Fig. 6(c) and (e)).



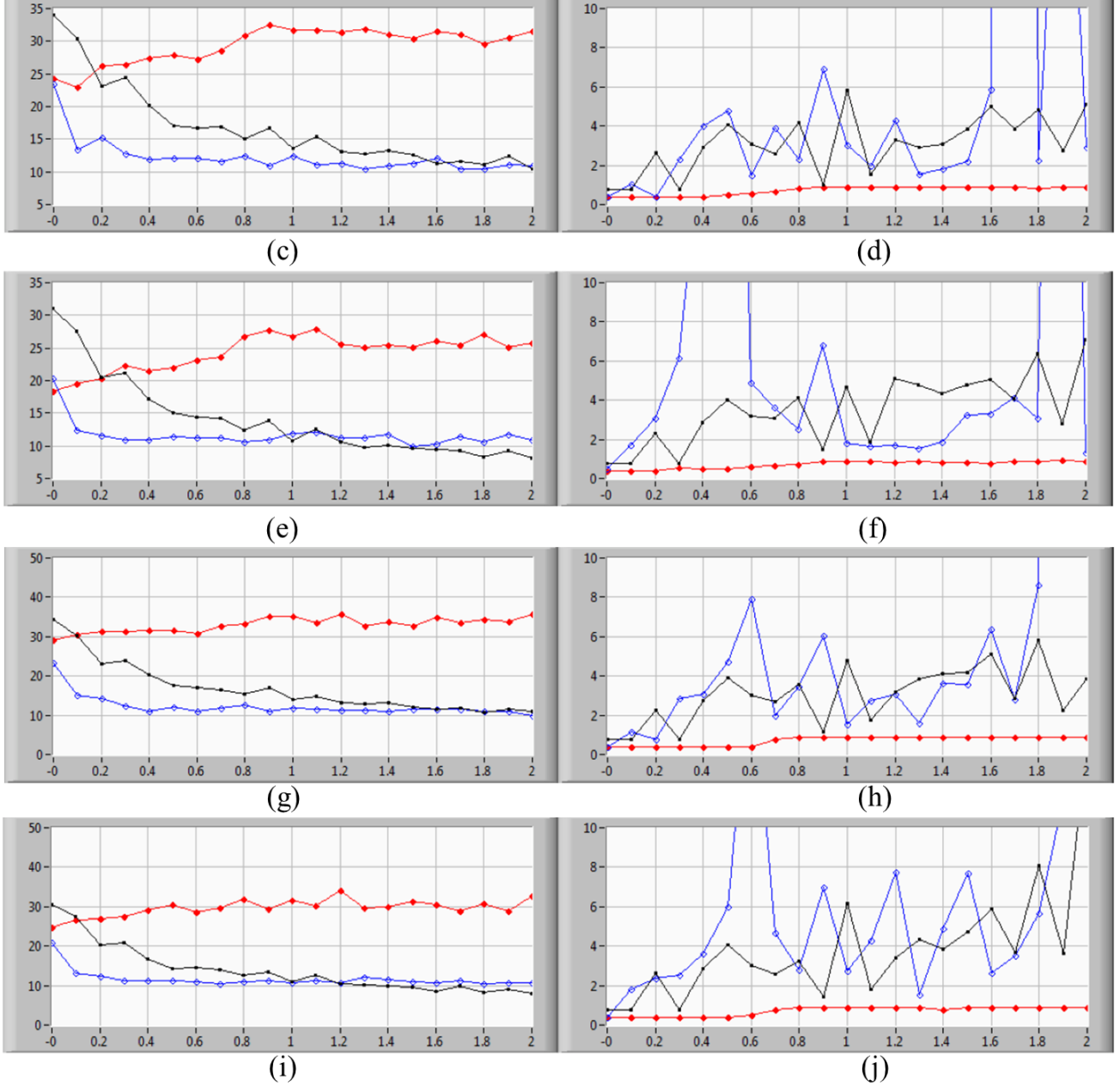


Figure 6. Comparisons of SNR (a, c, e, g, i) and FWHM (b, d, f, h, j) according to various parameters. Red: \hat{I}_h ; blue: I_h ; black: I_2 . (a) and (b): comparison according to the aperture size of L_T . (c)-(j): comparison according to a_ψ . For (c) and (d), $I_o = 0.1$ (intensity of object), $I_g = 1.0$ (intensity of guide-star), and $\eta = 2.5$. For (e) and (f), $I_o = 0.1$, $I_g = 1.0$, and $\eta = 5.0$. For (g) and (h), $I_o = 0.1$, $I_g = 10.0$, and $\eta = 2.5$. For (i) and (j), $I_o = 0.1$, $I_g = 10.0$, and $\eta = 5.0$.

4. CONCLUSION

We have proposed a SIDH AO scheme which can be applied for compensation of aberration which is present in an astronomical imaging. Because SIDH can record holographic information from the object whose illumination is completely incoherent, the guide-star hologram and full-field hologram can be recorded. With carefully designed parameters, SIDH system can achieve nice guide-star hologram which has proper information of aberration. Without aberration, the property of SIDH is easily predictable using theories studied so far. However, under the condition with

aberration, properties of SIDH AO are difficult to understand intuitively. As an aberration becomes severe, SNR of image reconstructed by SIDH AO does not degrade significantly, or even improves under a certain condition. This investigation implies that SIDH AO can be a useful tool for astronomical imaging.

ACKNOWLEDGMENT

The research reported in this publication was supported in part by the National Eye Institute of the National Institutes of Health under Award No. R21EY021876. The content is solely the responsibility of the authors and does not necessarily represent the official views of the National Institutes of Health.

REFERENCES

- [1] M. Hart, "Recent advances in astronomical adaptive optics," *Appl. Opt.* **49**(16), D17–D29 (2010).
- [2] K. M. Hampson, "Adaptive optics and vision," *J. Mod. Opt.* **55**(21), 3425-3467 (2008).
- [3] A. Roorda, F. Romero-Borja, W. J. Donnelly, H. Queener, T. J. Herbert, and M. C. W. Campbell, "Adaptive optics scanning laser ophthalmoscopy," *Opt. Express* **10**(9), 405–412 (2002).
- [4] R. J. Zawadzki, S. M. Jones, S. S. Choi, M. T. Zhao, B. A. Bower, J. A. Izatt, S. Choi, S. Laut, and J. S. Werner, "Adaptive-optics optical coherence tomography for high resolution and high-speed 3D retinal in vivo imaging," *Opt. Express* **13**(5), 8532–8546 (2005).
- [5] M. K. Kim, "Principles and techniques of digital holographic microscopy," *SPIE Reviews* **1**(1), 018005 (2010).
- [6] Y. Li, D. Abookasis, and J. Rosen, "Computer-generated holograms of three-dimensional realistic objects recorded without wave interference," *Appl. Opt.* **40**(17), 2864-2870 (2001).
- [7] T.-C. Poon, "Three-dimensional image processing and optical scanning holography," *Adv. Imag. Elect. Phys.* **126**, 329-350 (2003).
- [8] M. K. Kim, "Full color natural light holographic camera," *Opt. Express* **21**(8), 9636-9642 (2013).
- [9] J. Rosen and G. Brooker, "Non-scanning motionless fluorescence three-dimensional holographic microscopy," *Nat. Photonics* **2**(3), 190-195 (2008).
- [10] M. K. Kim, "Incoherent digital holographic adaptive optics," *Appl. Opt.* **52**(1), A117-A130 (2013).
- [11] J. Rosen, N. Siegel, and G. Brooker, "Theoretical and experimental demonstration of resolution beyond the Rayleigh limit by FINCH fluorescence microscopic imaging," *Opt. Express* **19**(27), 26249-26268 (2011).